LETTERS

Dust−climate couplings over the past 800,000 years from the EPICA Dome C ice core

F. Lambert[1,2], B. Delmonte[3], J. R. Petit[4], M. Bigler[1,5], P. R. Kaufmann[1,2], M. A. Hutterli[6], T. F. Stocker[1,2], U. Ruth[7], J. P. Steffensen[5] & V. Maggi[3]

Dust can affect the radiative balance of the atmosphere by absorbing or reflecting incoming solar radiation[1]; it can also be a source of micronutrients, such as iron, to the ocean[2]. It has been suggested that production, transport and deposition of dust is influenced by climatic changes on glacial−interglacial timescales[3–6]. Here we present a high-resolution record of aeolian dust from the EPICA Dome C ice core in East Antarctica, which provides an undisturbed climate sequence over the past eight climatic cycles[7,8]. We find that there is a significant correlation between dust flux and temperature records during glacial periods that is absent during interglacial periods. Our data suggest that dust flux is increasingly correlated with Antarctic temperature as the climate becomes colder. We interpret this as progressive coupling of the climates of Antarctic and lower latitudes. Limited changes in glacial−interglacial atmospheric transport time[4,9,10] suggest that the sources and lifetime of dust are the main factors controlling the high glacial dust input. We propose that the observed ∼25-fold increase in glacial dust flux over all eight glacial periods can be attributed to a strengthening of South American dust sources, together with a longer lifetime for atmospheric dust particles in the upper troposphere resulting from a reduced hydrological cycle during the ice ages.

The EPICA (European Project for Ice Coring in Antarctica) ice core drilled at Dome C (hereafter EDC) in East Antarctica ($75°06'$ S; $123°21'$ E) covers the past 800,000 yr (Fig. 1a). The dust flux record of Vostok (Fig. 1b) is thus extended over four additional cycles (Fig. 1c). The glacial–interglacial climate changes are well reflected in the sequence of high and low dust concentrations with typical values from 800 to $15\,\mu g\,kg^{-1}$ and a ratio of 50 to 1 over most of the past eight climate cycles. The concentration of insoluble dust in snow depends on a number of factors such as the primary supply of small mineral particles from the continents, which is related to climate and environmental conditions in the source region[11], the snow accumulation rate, the long-range transport, and the cleansing of the atmosphere associated with the hydrological cycle. The strontium and neodymium isotopic signature of dust[12] revealed that southern South America was the dominant dust source for East Antarctica during glacial times[13], although contributions from other sources are possible during interglacials[14]. Because of the low accumulation rate at Dome C ($\sim 3\,cm\,yr^{-1}$ water equivalent), dry deposition is dominant and the atmospheric dust load is best represented by the dust flux[15]. The total dust flux and the magnitude of the glacial–interglacial changes are remarkably uniform within the East Antarctic Plateau, as shown by the similarity between the EDC and the Vostok records (Fig. 1b, despite some chronological differences

and a 10-times finer resolution at EDC) over the past four climatic cycles and also depicted by the Dome Fuji dust record[16] (not shown).

At EDC, interglacials display dust fluxes similar to that of the Holocene ($\sim 400\,\mu g\,m^{-2}\,yr^{-1}$). However, some differences can be seen in the record before and after the Mid-Brunhes Event (MBE, $\sim 430\,kyr$ BP) which is considered a transition in the climatic record[7,8] from cooler (for example Marine Isotopic Stages, MIS 13, 15, 17) to warmer (for example MIS 11, 9 and 5.5) interglacials. Before the MBE there were fewer occurrences of low concentrations, and warm periods represent $\sim 12\%$ of the time, compared with $\sim 30\%$ after the MBE. All eight glacial periods appear similar in magnitude and show an average increase in dust flux by a factor of about 25, with glacial maxima displaying fluxes of at least $12\,mg\,m^{-2}\,yr^{-1}$. The weakest glacial stages in the EDC ice core are MIS 14 and 16. For MIS 14 this is consistent with the findings from terrestrial and marine records[6,17,18]. In contrast, MIS 16 in those records is the strongest glacial in the Late Quaternary period.

The extension of the EDC dust record to 800 kyr BP confirms the increased atmospheric dust load during cold periods of the Quaternary period with respect to warm stages. The first-order similarity of EDC dust with the global ice-volume record (Fig. 1e, $r^2 = 0.6$) confirms that major aeolian deflation in the Southern Hemisphere was linked to Pleistocene glaciations. Comparison with the magnetic susceptibility record of loess/palaeosol sequences from the Chinese Loess Plateau (Fig. 1f) also provides evidence for broad synchronicity of global changes in atmospheric dust load.

EDC dust has been measured using both a Coulter counter and a laser sensor (see Methods). Laser measurements are obtained at higher resolution along the core, but dust size is difficult to calibrate; therefore only the relative variation of the signal is used. Overall, the Coulter counter and laser (relative) size records (Fig. 1d) are in good agreement. The slight discrepancies during MIS 5.5, 6 and 12 are possibly related to the different sampling resolution, as size data from the laser and Coulter counter represent a continuous 1.1-m average and discrete 7-cm subsamples every 0.5–6 m, respectively. From MIS 14 ($\sim 2,900\,m$ depth) and downwards in the ice core, the dust size profile is not available because of the presence of particle aggregates formed in the ice. This phenomenon, which needs further investigation, has been observed in the EDC core only in very deep glacial sections, where ice thinning becomes very important and *in situ* temperature higher than $-8\,°C$ may allow partial melting around particles. This problem was solved through sonication of the samples, which allowed us to obtain reliable concentration data (see Methods). For the upper part of the record, larger (smaller) particles are generally observed during warm (cold) periods, as reflected by the
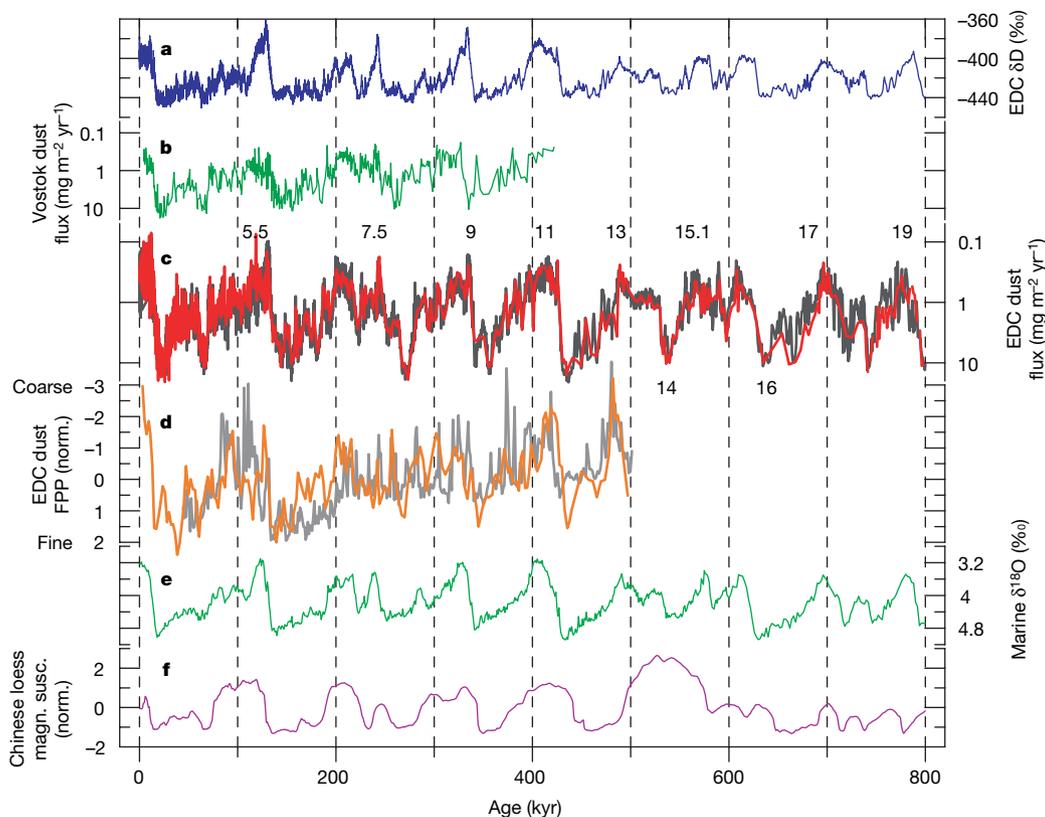
Figure 1 | EDC dust data in comparison with other climatic indicators.
a, Stable isotope (δD) record from the EPICA Dome C (EDC) ice core[8] back to Marine Isotopic Stage 20 (EDC3 timescale) showing Quaternary temperature variations in Antarctica. **b**, Vostok dust flux record (Coulter counter) plotted on its original timescale[11]. **c**, EDC dust flux records. Red and grey lines represent, respectively, Coulter counter (55-cm to 6-m resolution) and laser-scattering data (55-cm mean). Numbers indicate Marine Isotopic Stages. Note that the vertical extent of the scales of **b** and **c** is larger than for the other records. **d**, EDC dust size data expressed as FPP (see Methods). The orange and grey curves represent measurements by Coulter counter (2-kyr mean) and laser (1-kyr mean), respectively. **e**, Marine sediment δ^{18}O stack[18], giving the pattern of global ice volume. **f**, Magnetic susceptibility stack record for Chinese loess[17] (normalized).

variability in the fine particle percentage (FPP)[12], which is highest during the two last glacial periods. The advection of dust to central Antarctica involves the high levels of the troposphere and the small changes in dust size may reflect changes in the altitude of transport and thus transport time[12]. Higher FPP values in glacial times have been ultimately attributed to increased isolation of Dome C during glacials, in terms of reduced dust transport associated with greater subsidence[12] or possibly through baroclinic eddies.

Comparing dust and stable isotope (δD) profiles, there is a significant correlation during glacial periods (Fig. 2), and up to 90% of the dust variability can be explained by the temperature variations. In glacial periods, most of the δD events (for example, Antarctic Isotopic Maxima) have their counterparts in the dust data shown by a reduction of dust concentrations. In contrast, dust and temperature records are not correlated during interglacial periods (Fig. 2). Indeed, the (logarithmic) relationship between dust flux and δD can
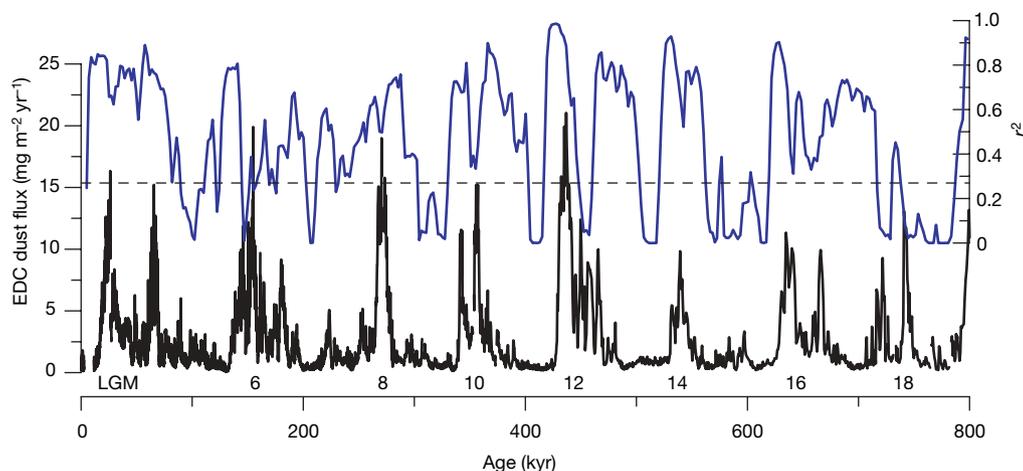

Figure 2 | EDC correlation between dust and temperature. Linear plot of dust flux (black) and the coefficient of determination r^2 (blue) between the high-pass filtered values (18-kyr cut-off) of both the δD and the logarithmic values of dust flux. The correlation was determined using 2-kyr mean values in both records and a gliding 22-kyr window. Correlations above $r^2 = 0.27$ (dashed line) are significant at a 95% confidence level. Numbers indicate the marine isotopic glacial stages.

be well fitted by a cubic polynomial (Fig. 3). Over the record, the geometric standard deviation from the polynomial fit represents a factor of ~2 in concentrations independent of the climatic period. Similarly, this relationship does not change before and after the MBE. The crescent shape of the dust–δD relationship suggests that the dust fluxes have a higher temperature sensitivity as the climate becomes colder. For δD values above about −405‰, Antarctic temperature and dust flux are not correlated, whereas there is a clear correlation for δD values below about −425‰. This behaviour may represent the expression of a progressive coupling between high- and low-latitude climate as temperatures become colder. During extreme glacial conditions the coupling appears as a direct influence of the Antarctic on the climate of southern South America[19,20]. The coupling of Antarctic and lower-latitude climate is probably coincident with the significantly extended sea ice over the Southern Atlantic and the Southern Ocean during glacials[21] and the consequent meridional (northward) shift of the atmospheric circulation (that is, the westerlies)[19–22].

Questions remain about the main factors influencing the high dust input into polar areas during glacial periods. So far, general circulation models[4,10] have reproduced a glacial dust transport and flux over tropical and mid-latitude regions which is in good agreement with global reconstructions[3], but they have failed to simulate the 25-fold increase observed in glacial dust input over Antarctica. This shortcoming is currently attributed to an incomplete representation of the source strength[23]. In addition, most of the models suggest modest changes in atmospheric transport[4,9,10], which seems supported by the relatively small changes in dust size in the EDC ice core, and by the comparison of the two EPICA ice cores[24]. Moreover, the suggestion that the 25-fold dust influx increase is mainly due to changes in source strength is challenged by evidence from South Atlantic marine records suggesting a 5- to 10-fold increase in the South American source strength[25,26] during the last glacial period.

On the basis of the new EDC data set, we suggest a new hypothesis for the glacial–interglacial changes in transport of dust. The indication (Fig. 3) that Antarctica and the southern low latitudes experienced a different coupling during the past 800 kyr is closely linked with the dust pathway within the high troposphere and the likely
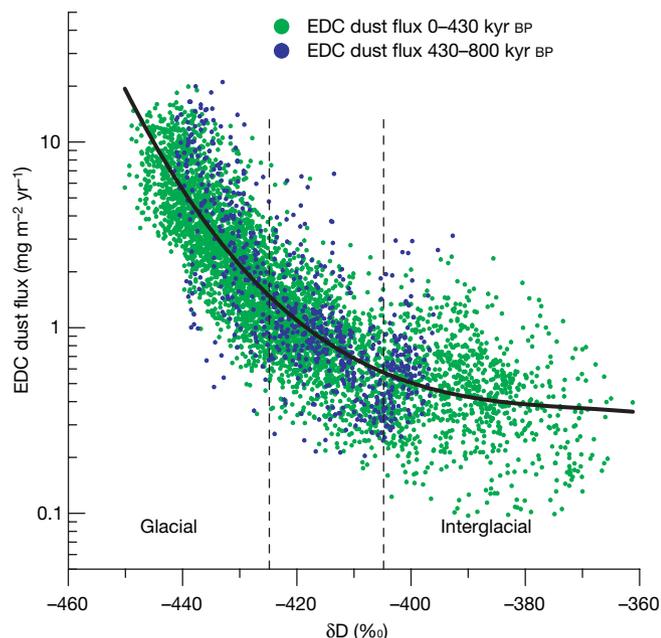
extended lifetime. With respect to the dust emitted from continents, the dust arriving in Antarctica, with a mode around 2 μm diameter[27], represents the endmember of the distribution. The small size of dust particles makes *en route* gravitational settling inefficient (very long dry deposition lifetime), allowing mixing and spreading at high altitude within the troposphere. The lifetime of the particles is primarily constrained by wet deposition[23,28] and therefore by water content and temperature. As an example, along a pathway 4–6 km high and with a mean temperature of about −40 °C (conditions similar to those observed over Antarctica), a temperature reduction by 5 °C, associated with a similar change of sea surface temperature over the Southern Ocean[29], reduces the saturation water vapour pressure to about half. Under such premises, a two-dimensional model[28] obtained an increase in dust flux to Antarctica of up to a factor of 5. Thus the roughly 25-fold increase in dust flux over the Antarctic plateau during glacials could be explained by a progressive coupling of the climate of Antarctic and lower latitudes with colder temperatures, one influencing the other, and leading to the stronger aeolian deflation of southern South America and to a significantly increased dust particle lifetime along their pathway in the high-altitude troposphere over the Southern Ocean. The new EDC data set thus provides important constraints for models of the dust cycle during glacial–interglacial cycles.

METHODS SUMMARY

Apparatus. Samples for Coulter Counter Multisizer IIe measurements were obtained from discrete samples (7 cm long), decontaminated at LGGE through washing in ultrapure water. We adopted the analytical procedure described in ref. 12 (and references therein). A total of about 1,100 values have been obtained.

We obtained laser scattering data from the University of Copenhagen device for the section between 0 and 770 m. The University of Bern device was used between 770 and 3,200 m. Data from both devices were calibrated by Coulter counter. Sampling resolution is about 1 cm.

Particle size distribution. Dust size is expressed as FPP. We define FPP according to ref. 12 as the proportion of the mass of particles having diameter between 1 and 2 μm with respect to the total mass of the sample, which typically includes particles in the size range 1 to 5 μm. This parameter is inversely correlated with the modal value of the log-normal dust mass (volume) size distribution.

From a depth of 2,900 m and below, some glacial samples show distributions with an anomalously large mode. This has been attributed to particle aggregate formation in ice (Supplementary Fig. 1) and prompted us to discard all size distribution data below that point until this phenomenon is better understood. To obtain reliable dust mass, samples were submitted to ultrasonic treatment to break the aggregates apart. Between 3,139-m and 3,190-m depth, 42 samples with anomalous size distribution were submitted to ultrasonic treatment. For 39 of these we accepted the new dust mass measurement, with 11 samples showing a significantly different mass value (Supplementary Table 1). Measurement on a few chosen samples above 3,139-m depth showed normal size distribution and concentration values. However, additional measurements are scheduled for in-depth analysis of the aggregate problem.

Figure 3 | EDC dust–temperature relationship. Values of δD (ref. 8) are plotted against dust flux (both at 55-cm resolution). Green and blue dots represent data from 0–430 kyr BP and 430–800 kyr BP, respectively. Superposed is a cubic polynomial fit,
$$\log_{10}(f) = -3.737 \times 10^{-6}(\delta D)^3 - 4.239 \times 10^{-3}(\delta D)^2 - 1.607(\delta D) - 204,$$
where f is the dust flux (mg m^{-2} yr^{-1}), and δD is in ‰ ($r^2 = 0.73$, $N = 5{,}164$).

1. Tegen, I. Modeling the mineral dust aerosol cycle in the climate system. *Quat. Sci. Rev.* **22**, 1821–1834 (2003).
2. Fung, I. *et al.* Iron supply and demand in the upper ocean. *Glob. Biogeochem. Cycles* **14**, 281–296 (2000).
3. Kohfeld, K. E. & Harrison, S. P. DIRTMAP: the geological record of dust. *Earth Sci. Rev.* **54**, 81–114 (2001).
4. Mahowald, N. *et al.* Dust sources and deposition during the last glacial maximum and current climate: A comparison of model results with paleodata from ice cores and marine sediments. *J. Geophys. Res.* **104**, 15895–15916 (1999).
5. Steffensen, J. P. The size distribution of microparticles from selected segments of the Greenland Ice Core Project ice core representing different climatic periods. *J. Geophys. Res.* **102**, 26755–26763 (1997).
6. Sun, Y. B., Clemens, S. C., An, Z. S. & Yu, Z. W. Astronomical timescale and palaeoclimatic implication of stacked 3.6-Myr monsoon records from the Chinese Loess Plateau. *Quat. Sci. Rev.* **25**, 33–48 (2006).
7. EPICA community members. Eight glacial cycles from an Antarctic ice core. *Nature* **429**, 623–628 (2004).
8. Jouzel, J. *et al.* Orbital and millennial Antarctic variability over the last 800 000 years. *Science* **317**, doi:10.1126/science.1141038 (2007).
9. Krinner, G. & Genthon, C. Tropospheric transport of continental tracers towards Antarctica under varying climatic conditions. *Tellus* **55B**, 54–70 (2003).

10. Werner, M. *et al.* Seasonal and interannual variability of the mineral dust cycle under present and glacial conditions. *J. Geophys. Res.* **107,** doi:10.1029/2002JD002365 (2002).

11. Petit, J. R. *et al.* Climate and atmospheric history of the past 420,000 years from the Vostok ice core, Antarctica. *Nature* **399,** 429–436 (1999).

12. Delmonte, B. *et al.* Dust size evidence for opposite regional atmospheric circulation changes over east Antarctica during the last climatic transition. *Clim. Dyn.* **23,** 427–438 (2004).

13. Lunt, D. J. & Valdes, P. J. Dust transport to Dome C, Antarctica at the Last Glacial Maximum and present day. *Geophys. Res. Lett.* **28,** 295–298 (2001).

14. Revel-Rolland, M. *et al.* Eastern Australia: A possible source of dust in East Antarctica interglacial ice. *Earth Planet. Sci. Lett.* **249,** 1–13 (2006).

15. Wolff, E. *et al.* Southern Ocean sea-ice extent, productivity and iron flux over the past eight glacial cycles. *Nature* **440,** 491–496 (2006).

16. Fujii, Y., Kohno, M., Matoba, S., Motoyama, H. & Watanabe, O. A 320 k-year record of microparticles in the Dome Fuji, Antarctica ice core measured by laser-light scattering. *Mem. Natl Inst. Polar Res.* **57,** 46–62 (2003).

17. Kukla, G., An, Z. S., Melice, J. L., Gavin, J. & Xiao, J. L. Magnetic susceptibility record of Chinese Loess. *Trans. R. Soc. Edinb. Earth Sci.* **81,** 263–288 (1994).

18. Lisiecki, L. E. & Raymo, M. E. A. Pliocene–Pleistocene stack of 57 globally distributed benthic delta O-18 records. *Paleoceanography* **20,** 1–17 (2005).

19. Iriondo, M. Patagonian dust in Antarctica. *Quat. Int.* **68,** 83–86 (2000).

20. Markgraf, V. *et al.* Paleoclimate reconstruction along the Pole−Equator−Pole transect of the Americas (PEP 1). *Quat. Sci. Rev.* **19,** 125–140 (2000).

21. Gersonde, R., Crosta, X., Abelmann, A. & Armand, L. Sea-surface temperature and sea ice distribution of the Southern Ocean at the EPILOG Last Glacial Maximum: A circum-Antarctic view based on siliceous microfossil records. *Quat. Sci. Rev.* **24,** 869–896 (2005).

22. Stuut, J.-B. W. & Lamy, F. Climate variability at the southern boundaries of the Namib (southwestern Africa) and Atacama (northern Chile) coastal deserts during the last 120,000 yr. *Quat. Res.* **62,** 301–309 (2004).

23. Mahowald, N. M. *et al.* Change in atmospheric mineral aerosol in response to climate: Last glacial period, preindustrial, modern, and doubled carbon dioxide climates. *J. Geophys. Res.* **111,** doi:10.1029/2005JD006653 (2006).

24. Fischer, H. *et al.* Reconstruction of millennial changes in dust emission, transport and regional sea ice coverage using the deep EPICA ice cores from Atlantic and Indian Ocean sector of Antarctica. *Earth Planet. Sci. Lett.* **260,** 340–354 (2007).

25. Kumar, N. *et al.* Increased biological productivity and export production in the glacial Southern Ocean. *Nature* **378,** 675–680 (1995).

26. Chase, Z. & Anderson, R. F. Evidence from authigenic uranium for increased productivity of the glacial Subantarctic Ocean. *Paleoceanography* **16,** 468–478 (2001).

27. Delmonte, B., Petit, J.-R. & Maggi, V. Glacial to Holocene implications of the new 27000-year dust record from the EPICA Dome C (East Antarctica) ice core. *Clim. Dyn.* **18,** 647–660 (2002).

28. Yung, Y. L., Lee, T., Wang, C. H. & Shieh, Y. T. Dust: A diagnostic of the hydrologic cycle during the last glacial maximum. *Science* **271,** 962–963 (1996).

29. Stenni, B. *et al.* A late-glacial high-resolution site and source temperature record derived from the EPICA Dome C isotope records (East Antarctica). *Earth Planet. Sci. Lett.* **217,** 183–195 (2004).